

See discussions, stats, and author profiles for this publication at: <https://www.researchgate.net/publication/252217919>

Low-field expressions for reversing-pulse electric birefringence of ionized polyions with permanent, ionic, and electronic dipole moments: A further extension of the ion-fluctuatio...

ARTICLE *in* THE JOURNAL OF CHEMICAL PHYSICS · NOVEMBER 1996

Impact Factor: 2.95 · DOI: 10.1063/1.472733

CITATIONS

7

READS

6

3 AUTHORS, INCLUDING:



Ryo Sasai

Shimane University

119 PUBLICATIONS 1,314 CITATIONS

SEE PROFILE

Low-field expressions for reversing-pulse electric birefringence of ionized polyions with permanent, ionic, and electronic dipole moments: A further extension of the ion-fluctuation theory and the application to poly(α ,L-glutamic acid)

Kiwamu Yamaoka,^{a)} Ryo Sasai, and Kazuhiro Kohno

Department of Materials Science, Faculty of Science, Hiroshima University, 1-3-1 Kagamiyama, Higashi-Hiroshima 739, Japan

(Received 23 July 1996; accepted 13 August 1996)

A rigorous theory was further extended for the reversing-pulse electric birefringence (RPEB) of the ionized polyion of cylindrical symmetry with the permanent dipole moment μ_3 , in addition to two previously considered electric dipole moments, i.e., the root-mean-square-average moment $\langle m_3^2 \rangle^{1/2}$ resulting from the fluctuation of ion-atmosphere along the longitudinal (3)axis of the polyion with a single relaxation time τ_I , as originally proposed by Szabo *et al.* [J. Chem. Phys. **85**, 7472 (1986)], and the electronic moment from the intrinsic covalent polarizability anisotropy $\Delta\alpha$ between the longitudinal and transverse axes of the polyion by Yamaoka *et al.* [J. Chem. Phys. **101**, 1625 (1994)]. The extended RPEB expressions were derived with three electric and hydrodynamic parameters ($p = \mu_3^2/kT\Delta\alpha$, $q = \langle m_3^2 \rangle^{1/2}/kT\Delta\alpha$, and $\tau^* = \tau_I/\tau_\theta$) in the Kerr-law region. Calculated with appropriate values to these parameters, the theoretical curves show such new features that either maxima or minima appear in the buildup and reverse processes. The present theory was used to analyze a set of experimental RPEB signals of poly(α ,L-glutamic acid) in helical conformation in methanol and in methanol-water containing sodium hydroxide. By fitting the observed data to theoretical curves, the contribution of $\langle m_3^2 \rangle^{1/2}$ was shown to surpass that of μ_3 for the same helical sample that was partially ionized by neutralization with sodium hydroxide. © 1996 American Institute of Physics. [S0021-9606(96)50943-8]

I. INTRODUCTION

Electric birefringence has been shown to be a useful technique to study the electric, optical, and hydrodynamic properties and the field-orientational dynamics of ionized or unionized polymers of diverse structures.¹⁻⁵ The reversing-pulse electric birefringence (hereafter abbreviated as RPEB) method was first developed by O'Konski and his co-workers,^{6,7} and its theory was formulated by Tinoco and Yamaoka.⁸ A new theory on RPEB was recently developed by Szabo *et al.* for rodlike polyions.⁹ This (SHE) theory is new in that the field orientation is solely due to the root-mean-square-averaged electric dipole moment resulting from the distortion of ion-atmosphere surrounding a cylindrically symmetric polyion molecule, and in that the relaxation time resulting from the fluctuation of counterions in the ion-atmosphere is coupled with the rotational relaxation time of the whole molecule. The SHE theory was extended by Yamaoka *et al.* to explicitly include the intrinsic polarizability anisotropy of a polyion and, hence, suited for studying the field orientation behavior of the polyion which is associated with the field-induced electric moment besides the ion fluctuation.¹⁰ This extended (YTS) theory was applied to explain the RPEB signal of disklike montmorillonite particles suspended in aqueous media.¹⁰

The present paper aims at further extending the YTS theory to include the effect of the permanent dipole moment of a polyion on observed RPEB signal patterns. This newly

derived theoretical expression can be used to quantitatively analyze the RPEB signal of cylindrically symmetric and ionized polyion with the permanent, ionic, and covalent (electronic) moments. Such polyions include many structurally ordered polypeptides and proteins like α -helices^{11,12} and triple-stranded collagen,¹³ which are inherently associated with the permanent dipole moment of large magnitude due to the backbone conformation. As an application of the present theory, a simulation was carried out on the experimental RPEB profile of unionized and partially ionized poly(α ,L-glutamic acid) in helical conformation.

II. THEORY

A. Potential

Let us consider a cylindrically symmetric polyion molecule, for which the symmetry axis is designated as the 3 axis and the perpendicular axis as the 1(=2) axis. A polyion solution is so dilute that no interaction exists between polyions. Based on the coupled rotational and ion-atmosphere dynamics,^{9,10} the total potential W of the polyion experienced by an external pulsed electric field $E(t)$ may be given as follows:

$$W(\delta_3, \theta) = \frac{n^2 e^2 \delta_3^2}{2\alpha_3} - n e \delta_3 E(t) \cos \theta - \frac{E(t)^2}{2} (\alpha_{33} - \alpha_{11}) \cos^2 \theta - \mu_3 E(t) \cos \theta, \quad (1)$$

^{a)} Author to whom correspondence should be addressed.

where θ is the angle between the electric field direction and the longitudinal axis of the polyion; δ_3 is the instantaneous displacement between the centers of the charge distribution of the polyion and the ion-atmosphere along the symmetry axis of the polyion, $\alpha_3 (= n^2 e^2 \langle \delta_3^2 \rangle / kT)$ is the ion-atmosphere polarizability of the polyion responsible for the electric moment $m_3 (= ne\delta_3)$ due to the ion fluctuation; n is the number of ionized groups on the polyion; e is the elementary charge; k is the Boltzmann constant; T is the absolute temperature. In the present treatment, the transverse distortion is not considered. The last term in Eq. (1) is newly added in the present work to incorporate the effect of the permanent dipole moment along the symmetry axis (μ_3) of a polyion on the field orientation. While the first two terms in Eq. (1) were introduced in the original formalism by Szabo *et al.*,⁹ the third term was added in the previous work by Yamaoka *et al.*,¹⁰ by considering the contribution of the anisotropy of the intrinsic polarizabilities (α_{33} and α_{11}) of a polyion to field orientation.

B. Diffusion equation in the orienting field

As in the previous case, the joint probability distribution function is given as $f(x, y, t)$, where $y = (m_3^2 / 2\alpha_3 kT)^{1/2}$ and $x = \cos \theta$. The rotational diffusion equation is given as⁹

$$\frac{\partial f(x, y, t)}{\partial t} = \Theta \frac{\partial}{\partial x} \left[(1 - x^2) \left(\frac{\partial}{\partial x} + \frac{1}{kT} \frac{\partial W}{\partial x} \right) f(x, y, t) \right] + \frac{n^2 e^2}{2\alpha_3 kT} D_I \frac{\partial}{\partial y} \left[\left(\frac{\partial}{\partial y} + \frac{1}{kT} \frac{\partial W}{\partial y} \right) f(x, y, t) \right], \quad (2)$$

where Θ is the rotary diffusion coefficient of the whole molecule around the transverse axis with the rotational relaxation time $\tau_\theta (= 1/6\Theta)$, W is given in Eq. (1), D_I is the translational diffusion coefficient of ion-atmosphere along the symmetry axis and equivalent to the relaxation time $\tau_I (= \alpha_3 kT / n^2 e^2 D_I)$. The joint distribution function was expanded in a series of the product of the Legendre $P_i(x)$ and Hermite $H_j(y)$ polynomials⁹

$$f(x, y, t) = \frac{1}{\sqrt{\pi}} \left[\sum_{i,j=0}^{\infty} a_{ij}(t) P_i(x) H_j(y) e^{-y^2} \right]. \quad (3)$$

Substituting Eqs. (1) and (3) to Eq. (2) and neglecting the terms higher than $E(t)^2$, the following general differential equation is obtained to solve for coefficients a_{ij} :

$$\begin{aligned} \frac{\partial a_{ij}(t)}{\partial t} = & - \left[i(i+1)\Theta + 2\eta E^2 \Theta \left\{ \frac{i(i+1)^2}{(2i+3)(2i+1)} - \frac{i^2(i+1)}{(2i+1)(2i-1)} \right\} + j\tau_I^{-1} \right] a_{ij}(t) + \epsilon E \Theta i(i+1)(j+1) \left[\frac{a_{i-1,j+1}(t)}{2i-1} \right. \\ & \left. - \frac{a_{i+1,j-1}(t)}{2i+3} \right] + \frac{\epsilon E(i+1)}{2(2i+3)} [\tau_I^{-1} - \Theta i] a_{i+1,j-1}(t) + \frac{\epsilon E i}{2(2i-1)} [(i+1)\Theta + \tau_I^{-1}] a_{i-1,j-1}(t) - 2\eta E^2 \Theta i(i+1) \\ & \times \left[\frac{(i+2)a_{i+2,j}(t)}{(2i+3)(2i+5)} - \frac{(i-1)a_{i-2,j}(t)}{(2i-3)(2i-1)} \right] - \frac{\mu E}{kT} [\Theta i(i+1)] \left[\left(\frac{1}{2i+3} \right) a_{i+1,j}(t) - \left(\frac{1}{2i-1} \right) a_{i-1,j}(t) \right], \end{aligned} \quad (4)$$

where $\epsilon = (2\alpha_3/kT)^{1/2}$ and $\eta = \Delta\alpha/2kT$. [Note that two errors in Eq. (4) of Ref. 10 are now corrected.]

The coefficient $a_{00}(t) = 1/2$, and others, $a_{10}(t)$, $a_{11}(t)$, and $a_{20}(t)$, are evaluated by solving the simultaneous differential equations of Eq. (4) for indices $i = (0, 2)$ and $j = (0, 1)$. By substituting these coefficients, the final form of $a_{20}(t)$ is given as

$$\begin{aligned} a_{20}(t) = & \left(\frac{\beta}{2} \right)^2 e^{-2\Theta t} + \left(\frac{\Theta \tau_I}{4\Theta \tau_I - 1} \right) \rho^2 e^{-(2\Theta + \tau_I^{-1})t} \\ & + \left\{ \left(\frac{\beta}{2} \right)^2 + \left(\frac{\Theta \tau_I}{4\Theta \tau_I - 1} \right) \rho^2 - \frac{1}{6}(\beta^2 + \rho^2 \right. \\ & \left. + 2\gamma) \right\} e^{-6\Theta t} + \frac{1}{6}(\beta^2 + \rho^2 + 2\gamma), \end{aligned} \quad (5)$$

where $\beta = \mu_3 E / kT$, $\rho = (\alpha_3 / kT)^{1/2} E$, and $\gamma = \Delta\alpha E^2 / 2kT$. The initial conditions are $a_{11}(0) = 0$ and $a_{20}(0) = 0$

for the buildup process of electric birefringence and $a_{11}(0) = -a_{11}(\infty)$ and $a_{20}(0) = a_{20}(\infty)$ for the reverse process.

C. RPEB Expressions in the Kerr-law region

The time-dependent electric birefringence, $\Delta n(t)$, can be calculated with a single coefficient [Eq. (5)] for the Kerr-law region (up to E^2 terms)^{9,10}

$$\langle P_2[\cos \theta(t)] \rangle = \frac{2}{5} a_{20}(t). \quad (6)$$

Finally, the normalized birefringence for the buildup process $\Delta_B(t)$, defined as $\Delta n_B(t) / \Delta n_B(\infty)$, is derived for the case that $4\Theta \tau_I - 1 \neq 0$

$$\Delta_B(t) = 1 - \frac{3}{2} \left(\frac{p}{p+q+1} \right) e^{-2\Theta t} - \left(\frac{6\Theta \tau_I}{4\Theta \tau_I - 1} \right) \times \left(\frac{q}{p+q+1} \right) e^{-(2\Theta + \tau_I^{-1})t} - \left[1 - \frac{3}{2} \left(\frac{p}{p+q+1} \right) - \left(\frac{6\Theta \tau_I}{4\Theta \tau_I - 1} \right) \left(\frac{q}{p+q+1} \right) \right] e^{-6\Theta t}. \quad (7)$$

Similarly, the normalized birefringence for the reverse process $\Delta_R (= \Delta n_R(t)/\Delta n_R(\infty))$ is given as

$$\Delta_R(t) = 1 - \left(\frac{3p}{p+q+1} \right) e^{-6\Theta t} - \left(\frac{6\Theta \tau_I}{4\Theta \tau_I - 1} \right) \times \left(\frac{2q}{p+q+1} \right) e^{-(2\Theta + \tau_I^{-1})t} + \left[\frac{3p}{p+q+1} + \left(\frac{6\Theta \tau_I}{4\Theta \tau_I - 1} \right) \left(\frac{2q}{p+q+1} \right) \right] e^{-6\Theta t}. \quad (8)$$

In the case where $4\Theta \tau_I - 1 = 0$ (this case was missed in the previous SHE and YTS theories), which corresponds to $\tau_I/\tau_O = 1.5$, Eqs. (7)–(8) must be written as follows:

$$\Delta_B(t) = 1 - \frac{3}{2} \left(\frac{p}{p+q+1} \right) e^{-2\Theta t} - \left[1 - \frac{3}{2} \left(\frac{p}{p+q+1} \right) + (6\Theta t) \left(\frac{q}{p+q+1} \right) \right] e^{-6\Theta t}, \quad (9)$$

and

$$\Delta_R(t) = 1 - \left(\frac{3p}{p+q+1} \right) e^{-2\Theta t} + \left[\frac{3p}{p+q+1} - (6\Theta t) \times \left(\frac{2q}{p+q+1} \right) \right] e^{-6\Theta t}. \quad (10)$$

Finally, the normalized birefringence for the field-off decay process $\Delta_D (= \Delta n_D(t)/\Delta n_D(0))$ is given as

$$\Delta_D(t) = e^{-6\Theta t}, \quad (11)$$

where $p = \beta^2/2\gamma = \mu_3^2/kT\Delta\alpha$, $q = \rho^2/2\gamma = \langle m_3^2 \rangle/kT\Delta\alpha = \alpha_3/\Delta\alpha$, and $\langle m_3^2 \rangle (= n^2 e^2 \langle \delta_3^2 \rangle)$ is the mean-square-average electric dipole moment due to ion fluctuation along the symmetry axis.

Expressions (7)–(10), derived here for the buildup and reverse processes, now additionally contain the p terms, which were not present in the previous SHE and YTS formulas and originated with the permanent dipole moment. If no permanent dipole moment is present in a polyion ($p=0$), then Eqs. (7)–(8) reduce to Eqs. (10)–(11) of the YTS theory.¹⁰ If the ionic electric moment is present without permanent and electronic dipole moments ($\rho \neq 0$ but $\beta, \gamma=0$), then Eqs. (7)–(8) reduce exactly to those originally derived by Szabo *et al.* [cf. Eqs. (21)–(22) in Ref. 9]. If the ionic moment alone is absent ($\rho=0$ but $\beta, \gamma \neq 0$), the Eqs. (7)–(8) reduce to the classical expressions of the β, γ -mixed orientation first derived by Tinoco and Yamaoka.⁸ Since $q = \alpha_3/\Delta\alpha$, the ratio of the ion-fluctuation polarizability to the intrinsic polarizability anisotropy, the sign of q can be

either positive, zero, or negative, and so is the sign of p . Thus the present expressions (7)–(10) can be utilized for the quantitative analysis of diverse patterns of experimental RPEB signals.

In the Kerr-law region, the steady-state birefringence Δn ($t \rightarrow \infty$) is given by Eqs. (7)–(8) as

$$\Delta n(\infty) = n_{\parallel} - n_{\perp} = 2\pi C_v \left(\frac{\Delta g}{n} \right) \left(\frac{E^2}{15kT} \right) \times \left(\frac{\mu^2}{kT} + \frac{\langle m^2 \rangle}{kT} + \Delta\alpha \right), \quad (12)$$

where n_{\parallel} and n_{\perp} are the refractive indices of the macromolecular solution parallel and perpendicular to the direction of the electric field; C_v and Δg ($= g_3 - g_1$) are the volume fraction and the optical anisotropy factor of the solute, respectively; n is the refractive index of the solution in the absence of the field. The first term in the third parentheses of Eq. (12) now results from the contribution of the permanent dipole moment to birefringence, while the second and third terms originated from the previous theories.^{9,10}

III. EXPERIMENT

A. Materials

A purified poly(α ,L-glutamic acid), $(\text{Glu})_n$, sample with a weight-average degree of polymerization of 708 was used. The preparation of methanol-soluble $(\text{Glu})_n$ in the acid form was given elsewhere in detail.¹⁴ $(\text{Glu})_n$ solutions in the methanol and water mixed solvents (95:5 v/v%) were prepared by adding appropriate volume of water, which contained a minute amount of sodium hydroxide. The helical conformation of each solution was checked with far-uv circular dichroism.¹⁴

B. Measurements

RPEB measurements were performed at 20 °C and at 535 nm on an instrument, which was constructed in our laboratory and described in detail elsewhere.¹⁵

IV. RESULTS AND DISCUSSION

Theoretical RPEB curves can be calculated from Eqs. (7)–(11) with three parameters of p , q , and τ^* ($= \tau_I/\tau_O$) and may be plotted against the reduced time $6\Theta t$. With these parameters, a great number of theoretical curves can possibly be drawn to simulate observed signal patterns.

A. The case where humps or dips appear in the buildup and reverse

Figure 1 shows theoretical RPEB curves for negative values of p and q , for which the negative value of $\Delta\alpha$ is responsible, at fixed values of p ($= -0.5$) and τ^* ($= 1$). According to the present theory, a curve should show a large dip or hump each in the buildup and reverse processes, depending on the range of $p+q$. In the $-1 < p+q < 0$ range, a hump, but not a dip, appears each in the buildup and reverse. The humps develop exceedingly high, as the sum of p and q

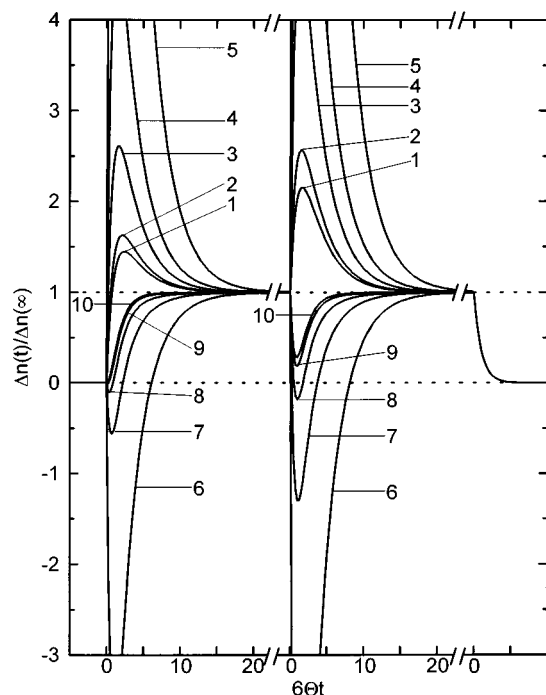


FIG. 1. Theoretical RPEB curves calculated with three parameters p , q , and τ^* for the cases, where the extrema appear in both buildup and reverse processes. The ordinate is the normalized birefringence, $\Delta n(t)/\Delta n(\infty)$ and the abscissa is the reduced time $6\Theta t$. Two parameters are fixed: $p = -0.5$ and $\tau^* = 1$. The parameter q is varied: 0 (curve 1), -0.1 (2), -0.3 (3), -0.4 (4), -0.47 (5), -0.6 (6), -1 (7), -2 (8), -5 (9), and -10 (10). Two dotted lines correspond to the base line and the normalized value of 1. The sign of steady-state birefringence $\Delta n(\infty)$ is negative for curves 1–5 but positive for curves 6–10, provided that $(\Delta g/n) > 0$ in Eq. (12).

approaches -1 from the less negative side. The hump in the reverse portion is always more distinct than that in the buildup. At $p + q = -1$, the RPEB curve diverges with infinitely high humps. The RPEB behavior of this type has not been observed experimentally as yet. In the range of $p + q < -1$, a dip appears each in the buildup and reverse processes. The depth of the dip becomes quite large, as the sum of p and q approaches -1 from the more negative side.

B. The case where a dip appears only in the reverse

Figure 2 shows theoretical RPEB curves calculated by varying values of p at fixed values of $q (=10)$ and $\tau^* (=1)$. With the increase in $p (>0)$, the dip in the reverse process becomes progressively deep, crossing over the base line [cf. curve (8) at $p = 100$]. Even if a polyion possesses no permanent dipole moment ($p = 0$), the RPEB signal should show a dip in the reverse, but the curve reaches the steady-state only monotonically with no inflection in the buildup, decaying exponentially upon field removal. This feature is associated only with positive values of both p and q , i.e., the positive value of $\Delta\alpha$.

C. The case where τ^* varies

Figure 3 shows another interesting case of RPEB curves, in which the parameter τ^* was varied at a fixed set of p and

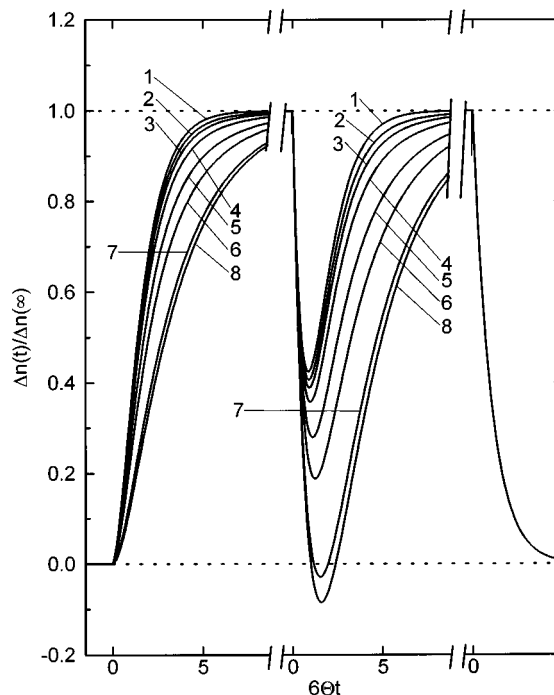


FIG. 2. Theoretical RPEB curves calculated for the case, where a dip appears only in the reverse process. Two parameters are fixed: $q = 10$ and $\tau^* = 1$. The parameter p is varied: 0 (curve 1), 0.5 (2), 1 (3), 2 (4), 5 (5), 10 (6), 50 (7), and 100 (8). $\Delta n(\infty) > 0$ in all cases.

q values. Theoretical curves indicate that the heights of humps are gradually lowered [Fig. 3(a)] and the depths of dips become shallower [Fig. 3(b)] with decreasing values of τ^* . If the ion–atmosphere relaxation time is fast, as compared with the overall molecular rotational relaxation ($\tau^* \rightarrow 0$), the height or depth is controlled by the value of p . The rise curves of RPEB signals in the buildup process are affected only moderately by 100-fold change in τ^* , but a considerable change appears in the reverse process. Therefore, the change in the relaxation time of ion fluctuation with, say, an increase in the dissociation of ionizable groups on a rigid polyion chain can easily be detected from RPEB signals in the reverse process (*vide post*).

D. Characteristics of theoretical RPEB curves

The relaxation time τ_I for the distortion of ion–atmosphere may be very fast ($\tau_I \approx 0$) or very slow ($\tau_I \approx \infty$). In two limiting cases, RPEB expressions (7)–(8) reduce to

$$\Delta_B(t) = 1 - e^{-6\Theta t} - \frac{3}{2} \left(\frac{p}{p+q+1} \right) (e^{-2\Theta t} - e^{-6\Theta t}), \quad (13)$$

$$\Delta_R(t) = 1 - \left(\frac{3p}{p+q+1} \right) (e^{-2\Theta t} - e^{-6\Theta t}), \quad (14)$$

for $\tau^* = 0$, and

$$\Delta_B(t) = 1 - e^{-6\Theta t} - \frac{3}{2} \left(\frac{p+q}{p+q+1} \right) (e^{-2\Theta t} - e^{-6\Theta t}), \quad (15)$$

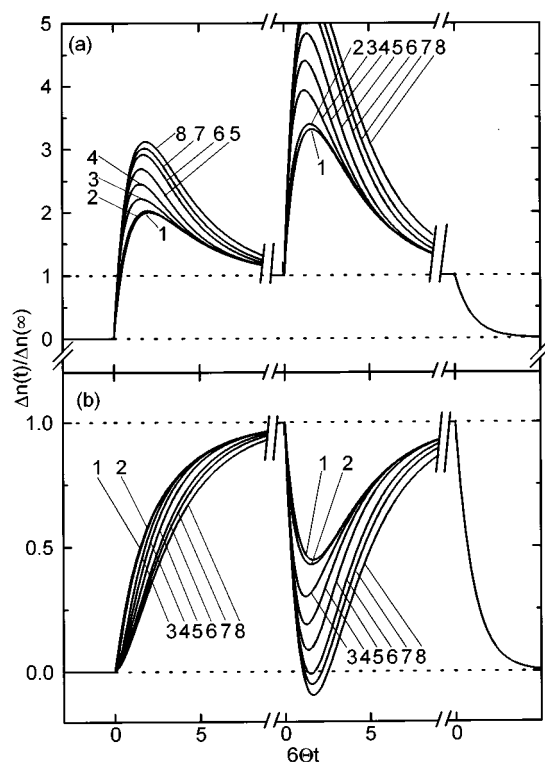


FIG. 3. The effect of the ratio of two relaxation times, τ^* , on the hump (a) and dip (b) of theoretical RPEB curves. The parameters are fixed: $p=q$ = -0.4 in (a) and $p=q=10$ in (b). Values of τ^* are varied: 0.01 (curve 1), 0.1 (2), 0.5 (3), 1 (4), 2 (5), 5 (6), 10 (7), and 100 (8) both in (a) and in (b).

$$\Delta_R(t) = 1 - 3 \left(\frac{p+q}{p+q+1} \right) (e^{-2\Theta t} - e^{-6\Theta t}), \quad (16)$$

for $\tau^* = \infty$. Equations (13)–(14) indicate that among three moments the permanent dipole moment mostly contributes to the RPEB transients for a fast fluctuation of ion–atmosphere. On the other hand, Eqs. (15)–(16) show that the ionic moment behaves just like a permanent dipole moment for the extremely slow fluctuation of ion–atmosphere.^{9,10} If the sum of these two dipole moments is written to be $p' \equiv p+q$ or $(\mu'_3 \equiv \mu_3 + \langle m_3^2 \rangle^{1/2})$, Eqs. (15)–(16) reduce to the β , γ -mixed dipole orientation originally formulated by Tinoco and Yamaoka.⁸

The areas of the normalized RPEB signals for the buildup (area B), reverse (area R), and decay (area D) processes, each of which was defined by the shaded portions, as shown in Fig. 4 of the previous paper,¹⁰ are derived by substituting $t' = 6\Theta t$ to Eqs. (9)–(11)

$$\begin{aligned} \text{Area B} &= \int_0^\infty [1 - \Delta_B(t')] dt' \\ &= \left(\frac{4(p+q)+1}{p+q+1} \right) \left(\frac{\tau^*}{\tau^*+3} \right) \\ &\quad + \left(\frac{4p+q+1}{p+q+1} \right) \left(\frac{3}{\tau^*+3} \right), \end{aligned} \quad (17)$$

$$\begin{aligned} \text{Area R} &= \int_0^\infty [1 - \Delta_R(t')] dt' = \left(\frac{6}{p+q+1} \right) \\ &\quad \times \left(p+q \left(\frac{\tau^*}{\tau^*+3} \right) \right), \end{aligned} \quad (18)$$

$$\text{Area D} = \int_0^\infty \Delta_D(t') dt' = 1. \quad (19)$$

The following area relation also holds in the present theory as in the previous one (in which the variable t should correctly be replaced by t'):¹⁰

$$\text{Area B} = \frac{1}{2}(\text{Area R}) + \text{Area D}. \quad (20)$$

This relationship has already been shown to hold for non-ionic polypeptide helices.¹⁶

Finally, the characteristic features appearing in the buildup and reverse processes of theoretical curves are summarized as follows (provided that $2\tau^* - 3 \neq 0$):

Features	Buildup	Reverse
Dip	$p+q < -1$	$p+q < -1; p>0, q>0,$
Hump	$-1 < p+q < 0$	$-1 < p+q < 0$
Monotonic rise	$p>0, q>0$	
No change		$p=q=0$

E. Comparison with experimental RPEB signal

Figure 4 shows some results of curve fitting for three experimental RPEB signals of $(\text{Glu})_n$ in the acid form, dissolved in pure methanol (a), and in methanol:water mixed solvents (b) and (c). The degree of neutralization of side-chain carboxyl groups, α_n , was increased to ca. 20% by adding an appropriate amount of sodium hydroxide. Since no change was observed in the circular dichroism spectra for these solutions, the helical content as well as the structure of $(\text{Glu})_n$ should remain unaltered in the 0%–20% range of α_n .¹⁴ Measured in the weak field region, where the Kerr law holds, the observed RPEB signal for unionized $(\text{Glu})_n$ in pure methanol exhibits a deep minimum only in the reverse process, the minimum being shallower with increasing α_n . Considering the rodlike nature of helical $(\text{Glu})_n$ with a large permanent dipole moment,¹⁴ the observed RPEB curves should be analyzed with Eqs. (7)–(8) for the positive values of p and q (cf. Fig. 2).

The experimental curve of the decay process was first analyzed with Eq. (11) to evaluate the rotational relaxation time τ_θ , and then the buildup and reverse processes were fitted by adjusting the parameters p , q , and τ^* . The best-fitted curves are shown with solid lines in Fig. 4 and the parameters are given in Table I. Both observed and calculated RPEB curves agree quite well under consideration of the polydispersity of the present $(\text{Glu})_n$ sample regarding the molecular weight.¹⁷ As judged from the τ^* value, the relaxation time for the distortion of ion–atmosphere containing sodium ions is much faster than the overall rotational relaxation time of the rodlike helix. By assuming that the covalent

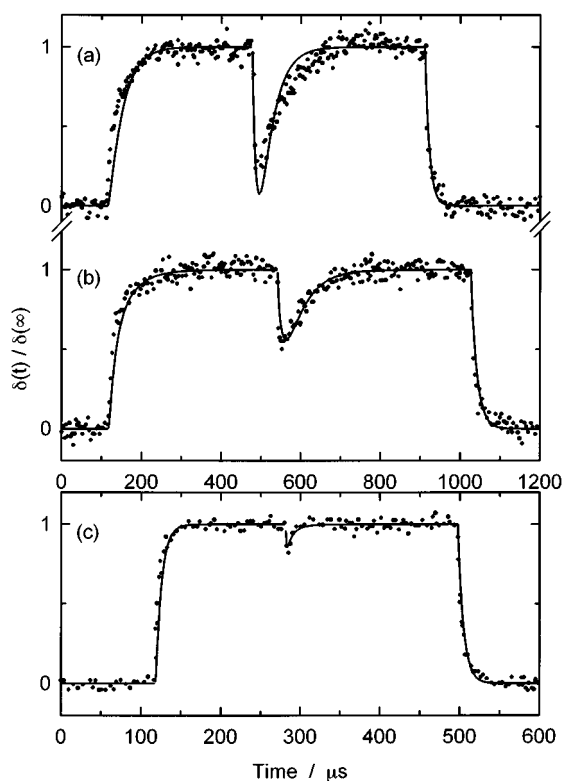


FIG. 4. RPEB signals of $(\text{Glu})_n$ measured in the methanol:water mixed solvent system and the fitting to theoretical curves. Solvents: (a) 100% methanol, (b) and (c) 95% methanol and 5% water in v/v. The degree of neutralization α_n and the applied electric field E in kV/cm are 0 and 3.75 in (a), 0.103 and 4.46 in (b), and 0.205 and 3.67 in (c). A 2 cm long Kerr cell with a 0.333 cm electrode gap was used. The residue concentration of $(\text{Glu})_n$, c in mM, is 1.95 in (a), 1.89 in (b) and (c). The ordinate is expressed with the optical phase retardation at time t normalized by the steady-state value, $\delta(t)/\delta(\infty)$. The specific retardation $\delta(\infty)/c$ in deg/mM is 0.27 (a), 0.35 (b), and 0.19 (c). The abscissa is expressed with observed time in μs . The actual sampling time between two successive dots was 0.5 μs , but the dots are averaged in this figure to reduce the numbers, so that a visual comparison between an observed signal and a calculated curve is made easier. Other experimental details are given elsewhere (Refs. 14 and 15).

anisotropy $\Delta\alpha$ remains constant both for unionized and ionized $(\text{Glu})_n$,¹⁴ values of the permanent dipole moment μ_3 and the ionic moment $\langle m_3^2 \rangle^{1/2}$ could be estimated (cf. Table I). As the ionization of side chain groups is increased, the contribution of the electric dipole moment $\langle m_3^2 \rangle^{1/2}$ to the field orientation becomes predominant. It should result from the ion fluctuation along the symmetry axis. These results all support the notion that the orientation mechanism of the partially ionized helical $(\text{Glu})_n$ polyion in the methanol: water mixed solvent system can be described by the present theory for the rodlike model, which takes into account three electric dipole moments.

V. CONCLUSION

By further extending the transient electric birefringence theory, first proposed by Szabo *et al.*⁹ on a basis of the polarization of ion-atmosphere, a useful set of RPEB expressions was derived for the ionized and regularly ordered polar polyion. The interaction between the applied electric field

TABLE I. Electro-optical and hydrodynamic parameters of $(\text{Glu})_n$ in helical conformation in pure methanol (a) and 95% methanol: 5% water mixed solvents (b), (c) are given in terms of the degree of neutralization, α_n . The parameters (p, q, τ^*) were evaluated from the simulation of RPEB signals. The rotational relaxation time τ_θ was estimated from the decay curve by the area method (Ref. 16). The permanent dipole moment μ_3 was calculated at 20 °C from $p = \mu_3^2/kT\Delta\alpha$ with $\Delta\alpha = 5.16 \times 10^{-33} \text{ Fm}^2$, which was evaluated from the field-strength dependence of steady-state birefringence for $(\text{Glu})_n$ in pure methanol (Ref. 14) and was assumed to be independent of α_n in three samples. 1 D = $3.336 \times 10^{-30} \text{ C m}$.

$(\text{Glu})_n$ Samples in	(a)	(b)	(c)
α_n	0.0	0.103	0.201
$p (= \beta^2/2\gamma)$	4	2.7	0.3
$q (= \rho^2/2\gamma)$	0	4	30
$\tau^* (= \tau_l/\tau_\theta)$	0	0.131	0.099
τ_θ (μs)	11	15.2	7.07
τ_l (μs)	0	2.0	0.7
μ (D)	2740	2250	750
$\langle m^2 \rangle^{1/2}$ (D)	0	2740	7510

and the permanent dipole moment was newly considered, in addition to the root-mean-square-averaged ionic electric moment due to the field-independent fluctuation of ion-atmosphere surrounding the polyion.

The new theoretical expressions with three parameters p , q , and τ^* may be used to explain a variety of RPEB signals. Humps (maxima) appear each in the buildup and reverse processes under the condition that $-1 < p + q < 0$, while dips (minima) appear each in these processes, provided that the condition $p + q < -1$ is fulfilled. These conditions imply that the covalent anisotropy of polarizabilities $\Delta\alpha$ intrinsic to the polyion is negative. If p and q are both positive, the RPEB signal shows only a minimum in the reverse process. In all cases, the smaller are the ratios of two relaxation times, τ^* , less distinct are these features in the RPEB patterns.

As an example, a set of theoretical curves ($p, q > 0$) was utilized to fit some experimental RPEB signal profiles of $(\text{Glu})_n$ samples in the helical conformation in solution. The electric and hydrodynamic parameters thus evaluated have led to the conclusion that the partially ionized polyion should be oriented by combined electric moments of permanent dipole, ion-atmosphere distortion, and intrinsic molecular polarizability anisotropy.

ACKNOWLEDGMENTS

The authors thank Mr. S. Yamamoto, a former student now at Mitsubishi Rayon Co., Ohtake, for his measuring RPEB signals of $(\text{Glu})_n$. This work was supported in part by Grants-in-Aid for Scientific Research (A) No. 02405008 and for Developmental Scientific Research (B) No. 06554031 from the Ministry of Education, Science, and Culture, Japan.

¹ *Molecular Electro-Optics*, Part 1 and Part 2, edited by C. T. O'Konski (Marcel Dekker, New York, 1976 and 1978).

² P. S. Stoylov, *Colloid Electro-Optics* (Academic, New York, 1991).

³ *Colloid and Molecular Electro-Optics 1991*, edited by B. R. Jennings and P. S. Stoylov (IOP, Bristol, 1992).

⁴ E. Fredericq and C. Houssier, *Electric Dichroism and Electric Birefringence* (Clarendon, Oxford, 1973).

- ⁵E. Charney, *Q. Rev. Biophys.* **21**, 1 (1988).
- ⁶C. T. O'Konski and A. J. Haltner, *J. Am. Chem. Soc.* **78**, 3604 (1956).
- ⁷C. T. O'Konski and R. M. Pytkowicz, *J. Am. Chem. Soc.* **79**, 4815 (1957).
- ⁸I. Tinoco, Jr. and K. Yamaoka, *J. Phys. Chem.* **63**, 423 (1959).
- ⁹A. Szabo, M. Haleem, and D. Eden, *J. Chem. Phys.* **85**, 7472 (1986).
- ¹⁰K. Yamaoka, M. Tanigawa, and R. Sasai, *J. Chem. Phys.* **101**, 1625 (1994).
- ¹¹K. Yamaoka, T. Ichibakase, K. Ueda, and K. Matsuda, *J. Am. Chem. Soc.* **102**, 5109 (1980).
- ¹²K. Yoshioka, M. Fujimori, K. Yamaoka, and K. Ueda, *Int. J. Macromol.* **4**, 55 (1982).
- ¹³K. Yamaoka, I. Kosako, and K. Gekko, *Polymer. J.* **21**, 107 (1989).
- ¹⁴K. Yamaoka, M. Kimura, and M. Okada, *Bull. Chem. Soc. Jpn.* **65**, 129 (1992).
- ¹⁵K. Yamaoka, S. Yamamoto, and I. Kosako, *Polymer. J.* **19**, 951 (1987).
- ¹⁶K. Yamaoka, S. Yamamoto, and K. Ueda, *J. Phys. Chem.* **89**, 5192 (1985).
- ¹⁷K. Yamaoka and K. Ueda, *J. Phys. Chem.* **86**, 406 (1982).